

Impact of sensitizer Yb and activator Tm on luminescence intensity of β -NaYF₄:Yb/Tm nanoluminophores

Sergey V. Kuznetsov^{1,a}, Sergey A. Burikov^{2,b}, Anna A. Fedyanina^{2,c}, Ekaterina A. Filippova^{2,d}, Vera Yu. Proydakova^{1,e}, Valerii V. Voronov^{1,f}, Nataliya Yu. Tabachkova^{1,g}, Pavel P. Fedorov^{1,h}, Tatiana A. Dolenko^{2,i}

¹Prokhorov General Physics Institute of the Russian Academy of Sciences, Moscow, 119991, Russia

²Department of Physics, Lomonosov Moscow State University, Moscow, 119991, Russia

^akouznetzovsv@gmail.com, ^bsergey.burikov@gmail.com, ^cfedyanechka@mail.ru,

^dfilippova.ea17@physics.msu.ru, ^evera.proydakova@gmail.com, ^fvoronov@lst.gpi.ru,

^gntabachkova@gmail.com, ^hppfedorov@yandex.ru, ⁱtdolenko@mail.ru

Corresponding author: Sergey V. Kuznetsov, kouznetzovsv@gmail.com

ABSTRACT In this study, the impact of sensitizer and activator ions concentration on the intensity of up-conversion luminescence of nanoluminophores β -NaYF₄:Yb³⁺/Tm³⁺ in dimethyl sulfoxide (DMSO) was investigated. Analysis of all luminescence spectral bands allows one to establish that the ratio of concentrations of ytterbium and thulium ions strongly effects on the luminescent properties of nanoluminophores. Increase of sensitizer concentration at constant activator concentration leads to an increase of the luminescence integral intensity. Optimal concentration of activators at fixed sensitizer concentration was determined: 2 mol.% for thulium and 18 mol.% for ytterbium. The sensitivity of each luminescence spectrum band to changes in the concentration of activators and sensitizers was explained by cross-relaxation processes in activator ions.

KEYWORDS up-conversion luminescence, nanoluminophores, rare earth elements, sensitizer, activator

ACKNOWLEDGEMENTS This research was performed according to the Development Program of the Interdisciplinary Scientific and Educational School of Lomonosov Moscow State University “Photonic and Quantum technologies. Digital medicine”. The study of the structure was carried out on the equipment of the Center Collective Use “Materials Science and Metallurgy” with the financial support of the Russian Federation represented by the Ministry of Education and Science (No. 075-15-2021-696).

FOR CITATION Kuznetsov S.V., Burikov S.A., Fedyanina A.A., Filippova E.A., Proydakova V.Yu., Voronov V.V., Tabachkova N.Yu., Fedorov P.P., Dolenko T.A. Impact of sensitizer Yb and activator Tm on luminescence intensity of β -NaYF₄:Yb/Tm nanoluminophores. *Nanosystems: Phys. Chem. Math.*, 2022, **13** (3), 331–341.

1. Introduction

Recently, nanoparticles based on various classes of chemical substances doped with ions of rare earth elements (REE) have attracted great interest due to their unique luminescent properties. In such nanoparticles, it is possible to implement up-conversion luminescence in which two or more photons with low energy turn into one photon with higher energy [1–3]. Such phosphors are used for optical imaging in biology and medicine [4–6], as optical coding elements [7], photovoltaic devices and anticounterfeiting [8], thermometry [9–12], and increasing the efficiency of solar panels [13–15].

Currently, the most effective up-conversion nanoluminophores have been developed on the basis of substances with gagarinite type crystal structure – NaYF₄ [9, 16, 17] or NaGdF₄ [5, 12, 18], which are doped with two types of ions. One (sensitizer ion) has a large absorption cross-section, and the other (activator ion) has high luminescence efficiency. The sensitizer ion absorbs the excitation energy and non-radiatively transfers it to the activator ion, which then emits up-conversion luminescence. Ytterbium ions often act as sensitizer while erbium, thulium, and holmium ions are used as activators [5, 8, 9, 12, 16–18].

The luminescent properties of nanoluminophores with REE ions are influenced by a number of factors such as intensity of exciting radiation [19–21], temperature [9–12], the ratio of concentrations of activator and sensitizer ions [5, 8, 17, 22–32], and environment of the emitting nanoparticles [33].

An increase of the sensitizer concentration leads to a significant increase of both the absorption cross-section and integral luminescence intensity [22, 23]. However, additional difficulties for the achieving the high-intensity luminescence arise from concentration quenching of luminescence [23], heating [34] and decrease of the luminescence lifetime due to the interactions between sensitizer and activator ions [24]. Luminescence concentration quenching at high concentrations of sensitizer ions can be eliminated by creating particles NaYF₄:Yb/Tm with sandwich-type multilayer architecture [23].

In this study, the concentration of sensitizer ions increased up to 60 % and the integral luminescence intensity continuously increased.

The luminescent properties of nanoluminophores with REE ions significantly depend on the concentration of activator ions. The Ho^{3+} , Tm^{3+} , and Er^{3+} ions were commonly used as activators due to cascade system of energy levels. The Yb^{3+} ions were used as sensitizers mostly often because of single excited state. In this regard, cross-relaxation processes between the ions are possible with appearance of the additional luminescence-quenching channel. As the concentration of activator ions increases accompanied by the simultaneous decrease of the distance between them the probability of excitation energy transfer to the unexcited ion increases as a result of electromagnetic interaction between them [25]. Such cross-relaxation converts both ions into intermediate state, which leads to cascade transfer of excitation energy to the vibrations of the crystal lattice [25].

The concentration of dopants (i.e., the average distance between neighboring active ions) has a great influence on the integral luminescence intensity and intensity ratio of the different peaks in the luminescence spectrum [26–32]. Increase of activator ions concentration (Er^{3+}) and probability of the cross-relaxation process (${}^4\text{S}_{3/2} + {}^4\text{I}_{15/2} \rightarrow {}^4\text{I}_{9/2} + {}^4\text{I}_{13/2}$) leads to decrease of the population of the ${}^4\text{S}_{3/2}$ level and increase of the population of the ${}^4\text{I}_{13/2}$ level [27]. Finally, the ${}^4\text{F}_{9/2}$ level is additionally populated from the ${}^4\text{I}_{13/2}$ level, which leads to increase of the intensity of the luminescence band in the red spectrum range. The probability of ${}^4\text{F}_{7/2} + {}^4\text{I}_{11/2} \rightarrow {}^4\text{F}_{9/2} + {}^4\text{F}_{9/2}$ cross-relaxation is also determined by the lifetimes of the corresponding levels and the concentration of Er^{3+} ions and affects the luminescence intensity in the red spectrum region [28]. Increase of the activator ions concentration (Er^{3+}) also leads to the increase of the probability of other cross-relaxation processes: ${}^2\text{H}_{11/2} + {}^4\text{I}_{15/2} \rightarrow {}^4\text{I}_{9/2} + {}^4\text{I}_{13/2}$ and ${}^4\text{I}_{11/2} + {}^4\text{I}_{13/2} \rightarrow {}^4\text{F}_{9/2} + {}^4\text{I}_{15/2}$ [29]. This leads to decrease of the luminescence intensity in the green spectrum region and increase of the luminescence intensity in the red spectrum region. Cross-relaxation mechanism (${}^4\text{F}_{7/2} + {}^4\text{I}_{11/2} \rightarrow {}^4\text{F}_{9/2} + {}^4\text{F}_{9/2}$) leads to the increase of the luminescence intensity in the red spectrum region relative to the luminescence in the green region at increase of the concentration of Yb^{3+} dopant ions [30]. Intensity of the luminescence bands in the blue (479 nm) and red (650 nm) spectral regions for $\text{NaYF}_4:\text{Yb}/\text{Tm}$ phosphors decreases with increasing thulium concentration from 0.1 to 2 % due to the presence of cross-relaxation processes [31]. Meanwhile, the band in the region of 800 nm turns out to be significantly less sensitive to changes of the concentration of thulium. Integral luminescence intensity, the intensity ratio of different spectral bands and the dependence of the luminescence intensity on the pump power for $\text{NaYF}_4:\text{Yb}/\text{Tm}$ phosphors are determined by the balance between the up-conversion of energy and excited state absorption dependent on dopant concentration [31].

For each crystal structure of the luminophores, the ion concentrations corresponding to maximal integral luminescence intensity were established [17,20,24,35–38]. The optimal concentrations of Yb^{3+} sensitizer and Er^{3+} activator ions for $\text{NaYF}_4:\text{Yb}/\text{Er}$ phosphors are 18 – 20 mol.% and less than 2 mol.%, respectively [36]. For $\text{NaYF}_4:\text{Yb}/\text{Tm}$ phosphors it has been demonstrated that the optimal concentration for excitation of maximal luminescence in the blue region of the spectrum is 20 – 30 mol.% for ytterbium and 0.3 mol.% for thulium [37]. Meanwhile, at least 30 mol.% ytterbium and 1 mol.% thulium are required to achieve the maximum luminescence intensity of the band in the region of 800 nm. Cross-relaxation processes at thulium concentrations larger than 2 mol.% for these phosphors already begin to significantly affect the intensity of the band in the region of 800 nm [38].

Thus, the concentrations of activator and sensitizer ions strongly impact on the luminescent properties of phosphors with REE ions. Therefore, the dependences of the nanoluminophores luminescence on the dopant ions concentrations are currently being actively investigated. However, there is a complicated problem in performing a comparative analysis and comparing the data from different authors for phosphors with nominally the same composition. The impossibility of the correct comparative analysis is caused by the fact that different authors studied nanoluminophores of the same nominal compositions prepared by different synthesis techniques from different initial chemicals. These nanoluminophores differed significantly in morphology and size. Moreover, laser radiation of various pump power density was used and only some of the most intense bands of the luminescence spectrum were analyzed.

Thus, in order to clarify the conclusions about the effect of the concentration of activators and sensitizers on the luminescent properties of up-conversion nanoluminophores, it is necessary to obtain complete luminescence spectra of nanoluminophores, differing from each other only in the concentrations of activators and sensitizers, under the same experimental conditions (intensity of excitation radiation, optical scheme of experiment etc.). Herewith, the nanoparticles should be synthesized by the same method using the same reagents.

In this article, the dependences of the intensity of the luminescence bands in spectral region 300 – 900 nm for the dispersions of $\beta\text{-NaYF}_4:\text{Yb}^{3+}/\text{Tm}^{3+}$ phosphors in dimethyl sulfoxide (DMSO) on the concentration of activator and sensitizer ions were recorded under the same experimental conditions. For this purpose, a series of samples differing in the concentration of activator and sensitizer ions were specially synthesized. As a result, the full luminescence spectra recorded under the same conditions at the same laser pumping power density were analyzed. The optimal concentration of activators at fixed sensitizer concentration is revealed, namely, it is 2 mol.% for thulium and 18 mol.% for ytterbium.

2. Materials and methods

2.1. Synthesis and characterization of the samples

Eight β -NaYF₄:Yb³⁺/Tm³⁺ nanoluminophores with different concentrations of ytterbium ions (sensitizer) and thulium (activator) were synthesised. Two series of β -NaYF₄:Yb³⁺/Tm³⁺ samples were synthesised with constant concentration of the sensitizer and varied concentration of activator and vice versa in the other series. Nanoparticles β -NaYF₄:Yb³⁺/Tm³⁺ were synthesized by the solvothermal synthesis technique in a high-boiling solvent according to the procedure described elsewhere [12, 39]. Ytterbium, thulium and yttrium acetates of purity 99.99 (Lanhit, Russia) were added to oleic acid (pure, Chimmed, Russia) and 90 % octadecene-1 (Sigma Aldrich). The reaction mixture was heated up to 130 °C under vigorous stirring under an argon atmosphere until completely dissolving of initial chemicals with preparing of ytterbium, thulium and yttrium oleates. The sub-product of reaction such as water and acetic acid were removed in vacuum. The sodium hydroxide and ammonium fluoride (chemically pure, Lanhit, Russia) were dissolved in methanol (chemically extra pure, Chimmed, Russia). Mixture of NaOH and NH₄F solutions was added to the reaction mixture with oleates at room temperature. Entire mixture was heated up to 50 – 60 °C and kept at this temperature for one hour with following removing methanol in vacuum. After removing the entire methanol, the reaction mixture was heated up to 315 °C stored for 3 hours and then cooled to 25 °C. The nanoparticle precipitate was separated from the solution by centrifugation (Eppendorf 5804 centrifuge, 6500 rpm, 5 min). The resulting nanoparticles were sequentially dispersed three times in chloroform and washed with 96 % ethanol. Suspensions of nanoparticles in DMSO (chemically pure, Chimmed, Russia) were prepared with the same concentration of 1 mg/ml according to the developed protocol: 10 ml of DMSO was added to 10 mg of β -NaYF₄:Yb/Tm nanoparticles. The resulting suspensions were sonicated at 35 kHz for 1 hour in the ultrasonic bath “GRAD 13-35”.

X-ray pattern diffraction of powders was performed on Bruker D8 diffractometer with CuK α -radiation. The typical X-ray pattern was corresponded to β -NaYF₄ crystal type (JCPDS card #16-0344, $a = 5.96$ Å, $c = 3.53$ Å, Fig. 1). Unit cell parameters of samples were evaluated by TOPAS software (Table 1).

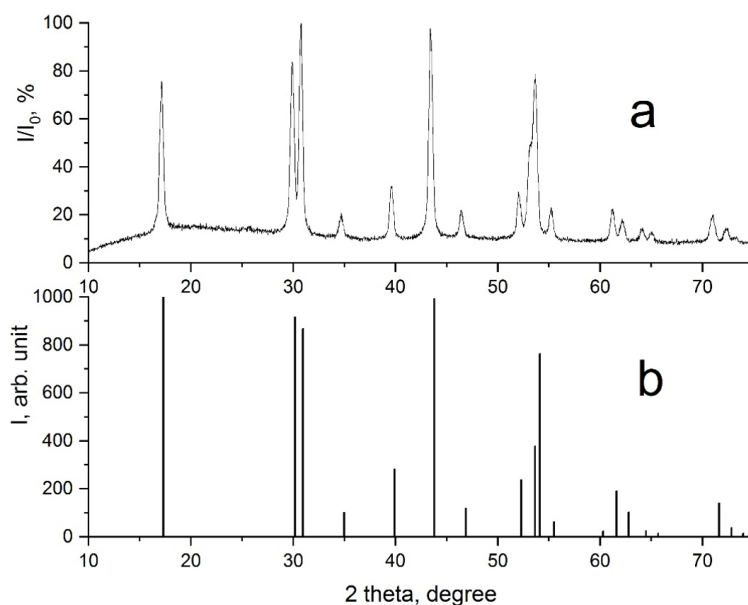


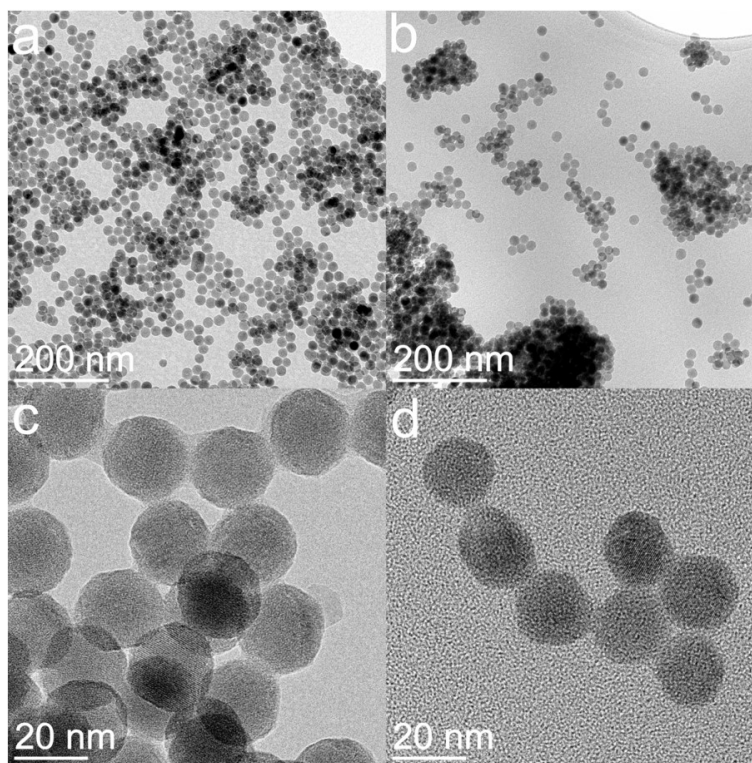
FIG. 1. X-ray pattern diffraction of β -NaYF₄:Yb(18 mol.):Tm(2 mol.) sample (a) and JCPDS # 16-0344 for β -NaYF₄ (b)

Transmission electron microscopy (TEM) was performed using JEOL JEM-2100 microscope. The particle size was estimated using the ImageJ software based on 50 particles (Table 1). TEM images of β -NaYF₄: Yb³⁺/Tm³⁺ samples are shown in Fig. 2 and Figs. A1–A3.

The nanoparticle sizes of β -NaYF₄: Yb³⁺/Tm³⁺ in DMSO suspensions were measured by dynamic light scattering (DLS) using Malvern Zetasizer Nano ZS setup (Table 1). The size distributions of nanoparticles in suspensions for several of the studied nanoluminophores are shown in Figs. A4–A6. As it follows from the obtained results, the sizes of most objects do not exceed 50 nm, which indicates that there is no significant aggregation of nanoparticles in suspensions. This is also evidenced by the observation of the colloidal stability of suspensions – for several months there was no precipitation of particles, and the luminescence intensity of complexes in suspensions did not decrease with time, which corresponds to the data we previously obtained [18].

TABLE 1. Characteristics of synthesized samples of $\beta\text{-NaYF}_4\text{:Yb}^{3+}/\text{Tm}^{3+}$

No	Composition	Unit cell parameters, Å	Size (TEM), nm	Size (DLS), nm
1	$\beta\text{-NaYF}_4\text{:Yb(10 %)/Tm(4 %)}$	$a = 5.9745(3)$ $c = 3.5196(1)$	16.7	21.2
2	$\beta\text{-NaYF}_4\text{:Yb(14 %)/Tm(4 %)}$	$a = 5.9734(4)$ $c = 3.5166(2)$	19.5	32.6
3	$\beta\text{-NaYF}_4\text{:Yb(18 %)/Tm(4 %)}$	$a = 5.9723(2)$ $c = 3.5134(1)$	22.8	38.1
4	$\beta\text{-NaYF}_4\text{:Yb(22 %)/Tm(4 %)}$	$a = 5.9717(5)$ $c = 3.5135(3)$	20.7	25.7
5	$\beta\text{-NaYF}_4\text{:Yb(18 %)/Tm(1 %)}$	$a = 5.9728(3)$ $c = 3.5153(2)$	18.9	36.4
6	$\beta\text{-NaYF}_4\text{:Yb(18 %)/Tm(2 %)}$	$a = 5.9731(3)$ $c = 3.5140(2)$	24.0	70.1
7	$\beta\text{-NaYF}_4\text{:Yb(18 %)/Tm(4 %)}$	$a = 5.9723(2)$ $c = 3.5134(1)$	22.8	50.5
8	$\beta\text{-NaYF}_4\text{:Yb(18 %)/Tm(6 %)}$	$a = 5.9707(1)$ $c = 3.5113(1)$	20.9	104.6

FIG. 2. TEM images of $\beta\text{-NaYF}_4\text{:Yb}^{3+}/\text{Tm}^{3+}$ nanoluminophores: No. 7 (left) and No. 8 (right)

2.2. Luminescent spectroscopy of $\beta\text{-NaYF}_4\text{:Yb}^{3+}/\text{Tm}^{3+}$ colloids in DMSO

A continuous diode laser with a wavelength of 980 nm (line width of 2 nm) and a pumping intensity of 205 W/cm² was used for excitation of the luminescence. Luminescence spectra were recorded in the spectral range of 300 – 900 nm at room temperature.

The samples were studied in the 90-degree geometry of the experiment in the standard quartz cuvette (10 × 10 × 50 mm). The registration system consisted of Acton 2500i monochromator (focal length 500 mm, diffraction grating 900 grooves per mm), and photomultiplier (Hamamatsu H-8259, operating in photon counting mode). A blocking interference filter was used to suppress the elastic scattering signal at the wavelength of 980 nm.

It occurs that the up-conversion luminescence in $\beta\text{-NaYF}_4\text{:Yb}^{3+}/\text{Tm}^{3+}$ samples is in accordance with the transitions scheme between the energy levels of ytterbium and thulium (Fig. 3).

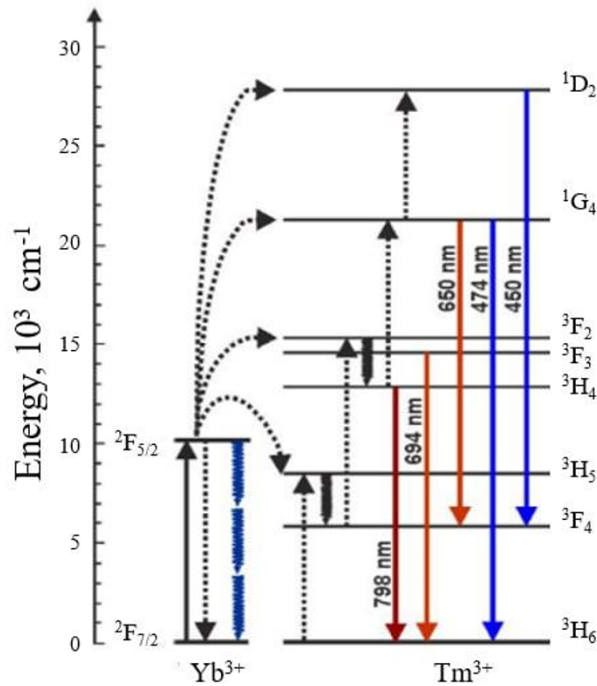


FIG. 3. Energy levels diagram and transitions demonstrating the generation of up-conversion radiation in β -NaYF₄:Yb³⁺/Tm³⁺ particles

The photon of the exciting radiation (980 nm) is absorbed by the ytterbium ion (transition ${}^2F_{7/2} \rightarrow {}^2F_{5/2}$) then the energy is transferred to the thulium ion according to transition ${}^3H_6 \rightarrow {}^3H_5$ with arising excited state. The energy of the next photon absorbed by the ytterbium ion allows the thulium ion to pass through the intermediate levels 3F_4 and 3F_2 to the level 3H_4 . From this level, radiative transition ${}^3H_4 \rightarrow {}^3H_6$ is possible with the emission of the photon with wavelength of 798 nm. Similarly (with the absorption of three or four photons), it is possible to populate levels 1G_4 and 1D_2 with radiative transitions causing up-conversion luminescence in the blue and red spectral regions (Fig. 3).

3. Results and discussion

3.1. Dependence of the intensity of up-conversion luminescence of nanoluminophores on the ratio between concentrations of activator and sensitizer

The recorded luminescence spectra for all the samples β -NaYF₄:Yb³⁺/Tm³⁺ in DMSO with the nanoparticle concentration (1 mg/ml) are presented in Fig. 4. Each spectrum contains a set of bands with various intensities corresponding to the following energy transitions: ${}^3H_4 \rightarrow {}^3H_6$ (798 nm), ${}^1G_4 \rightarrow {}^3H_6$ (474 nm), ${}^1D_2 \rightarrow {}^3F_4$ (450 nm), ${}^1G_4 \rightarrow {}^3F_4$ (650 nm), and ${}^3F_3 \rightarrow {}^3H_6$ (694 nm).

Luminescence intensity of nanoparticles with different ratio of concentrations of activator and sensitizer varies in a wide range (Fig. 4). Dependence of integral luminescence of nanoparticles on the concentration of sensitizer and activator ions is presented in Fig. 5.

Obtained results demonstrate the increase of integral luminescence at fixed activator concentration and increasing of sensitizer concentration (samples 1 – 4). Firstly, it can be explained by the fact that more energy of exciting radiation is absorbed. Secondly, it can be the result of the decrease of the average distance between activator and sensitizer ions with the increase of their concentration. Consequently, transmission of excitation from sensitizer ions to activator ions turns to be more effective.

The efficiency of energy transfer from sensitizer ions to activator ions is determined by the distance between sensitizer and activator ions (their concentrations) according to the formula [40, 41]:

$$P = \frac{1}{t_s} \left(\frac{R_0}{R} \right)^s, \quad (1)$$

where t_s is the effective lifetime of the excited state of sensitizer ion, that takes into account all the channels of deactivation except the energy transfer to activator ion; R is the distance between ions, which are involved into the energy transfer process; R_0 is the distance between ions when the rate of energy transfer equals the rate of the spontaneous decay of the excited state of sensitizer; s is the multipolar reaction index ($s = 6$ corresponds to dipole-dipole interaction, $s = 8$ – dipole-quadrupole, $s = 10$ – quadrupole-quadrupole). Increasing concentration of sensitizer ions leads to the decrease of R and the growth of efficiency of energy transfer to the activator ions.

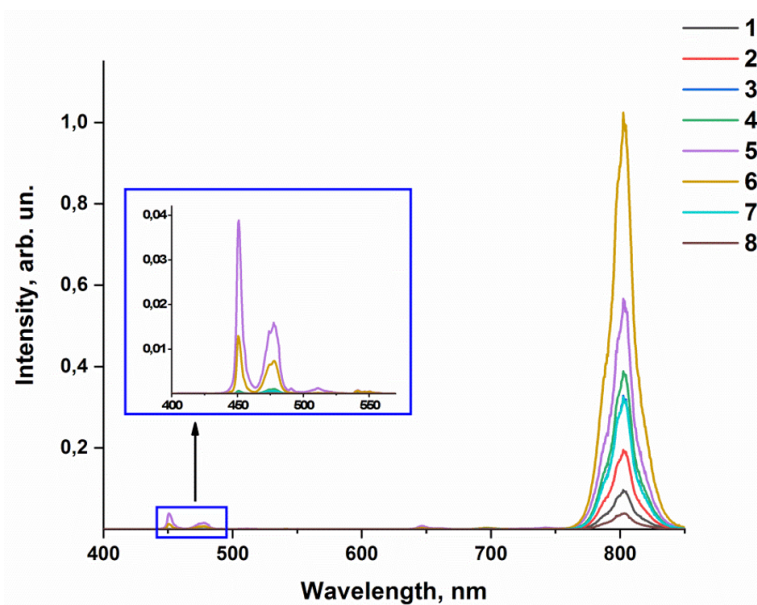


FIG. 4. Luminescence spectra of the studied samples No. 1 – 8

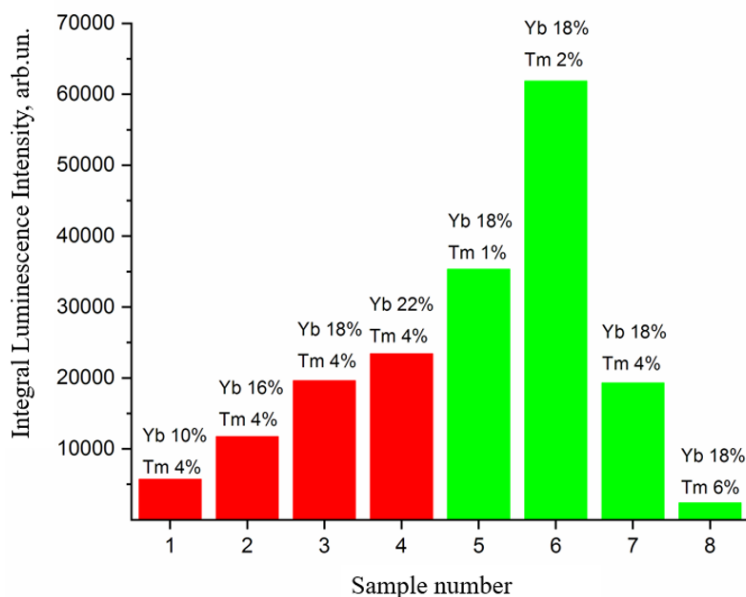


FIG. 5. Dependence of integral luminescence intensity on the concentration of sensitizer (Yb) and activator (Tm) ions

At fixed concentration of sensitizer ions (samples 5 – 8), the dependence of the luminescence intensity on the activator concentration is more complex. On the one hand, the increase of the activator concentrations leads to the increase of the luminescence intensity, since the number of luminescent centers is growing. On the other hand, the increase of the activators concentration may lead to the appearance of an additional luminescence quenching channel associated with the presence of cross-relaxation processes [17, 23]. Cross-relaxation is responsible for the concentration quenching of luminescence, since neighboring ions, one of which is in the excited state and the other in the ground state, exchange energy non-radiatively, as a rule, with subsequent relaxation of phonons [42].

Thus, there is a competition between the increase of the luminescence intensity due to the increase of the activator concentration and luminescence quenching due to cross-relaxation. This leads to the fact that there is an optimal concentration of activator ions at which the integral luminescence intensity is maximal. As it follows from the results obtained in this study, for the studied samples of $\beta\text{-NaYF}_4:\text{Yb}^{3+}/\text{Tm}^{3+}$ in DMSO such optimal concentration of Tm is 2 mol.% at the concentration of Yb 18 mol.% (Fig. 5).

It should be noted that the increase of the sensitizer concentration does not lead to deactivation of excited states due to cross-relaxation, since it requires the presence of several excited levels in the ion [23, 43].

3.2. Dependences of the intensities of the luminescence bands of nanoluminophores on the ratio of activator and sensitizer concentrations

The luminescence spectrum consists of the bands with different intensities (Fig. 4), therefore, the dependencies of the intensity on the concentration of activator and sensitizer ions for each band of the spectrum were constructed separately (Fig. 6).

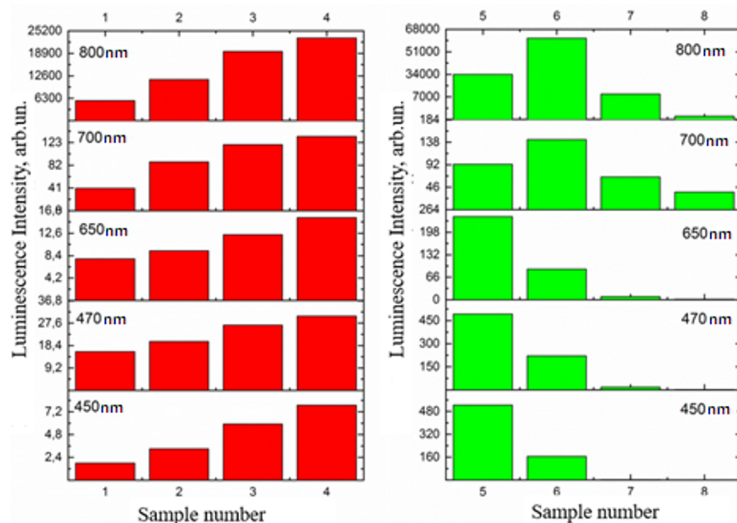


FIG. 6. Luminescence intensities of different bands while changing the concentration of sensitizer ions (left) and activator ions (right)

Samples with different sensitizer concentrations and fixed activator concentration have similar dependence, which has been previously revealed for integral intensity (Fig. 6, left). The increase of the sensitizer concentration leads to the increase of the luminescence intensity as the proportion of absorbed radiation increases and the distance between activator and sensitizers ions decreases, which causes the increase of the efficiency of energy transfer.

The results obtained for various concentrations of activator and fixed concentration of sensitizer are more complicated (Fig. 6, right). Dependences of the luminescence intensity on the concentration of the activator for the bands in the region of 700 and 800 nm qualitatively repeat the same dependences for integral intensity. Dependences of the luminescence intensity on the activator concentration for the bands in the regions of 450, 475 and 650 nm differ. The intensities of these bands decrease with the increase of the activator concentration.

Such a difference can be explained as follows. Different numbers of photons are required for excitation of the different bands of luminescence: excitation of bands in the regions of 700 and 800 nm requires two photons, 475 and 650 nm – three photons, 450 nm – four photons (Fig. 3). Therefore, bands with maximums at 450, 475 and 650 nm are more sensitive to the efficiency of cross-relaxation of excited states of activator ions.

Increasing activator concentration and decreasing average distance between ions resulted in increasing the probability of cross-relaxation. As a result, there is a monotonous decrease of the luminescence intensity of these bands with the increase of the concentration of the activator ions. It concerns especially the band in the region of 450 nm, which requires the largest number of photons for excitation. Its intensity decreases most rapidly with the increase of the concentration of activator ions (Fig. 6). Probably, the optimal value of the activator ion concentration for bands 450, 470, 650 nm corresponds to the thulium concentration of less than 1 mol.% with the fixed sensitizer concentration of 18 mol.%. At the same time, the optimal value of thulium concentration for bands with maximum in the region of 700 and 800 nm corresponds to 2 mol.%. Since the band in the region of 800 nm located in transparency tissue window makes the greatest contribution to the integral luminescence intensity (Fig. 6), the optimal value of the activator ion concentration for the integral luminescence intensity also equals 2 mol.%.

4. Conclusions

In this study, the dependences of the integral intensity and intensities of all bands of the luminescence spectra of β -NaYF₄:Yb³⁺/Tm³⁺ nanoluminophores in DMSO on the concentration of activator and sensitizer ions were investigated. In order to ensure the greatest reliability of the measured photophysical characteristics, a series of samples with different concentrations of activator and sensitizer ions were successfully synthesized. The spectra were recorded under the same optical scheme and intensity of excitation radiation.

It was established that the ratio between concentrations of ytterbium and thulium ions strongly influences on both the integral luminescence intensity and the intensity of individual spectral bands. The increase of the sensitizer concentration

at the constant concentration of the activator leads to the increase of the intensity of integral luminescence. At the fixed concentration of sensitizer ions, there is optimal activator concentration that provides the most intense luminescence. For the studied samples of $\beta\text{-NaYF}_4\text{:Yb}^{3+}/\text{Tm}^{3+}$ in DMSO, such optimal concentration of Tm is 2 mol.% at the concentration of Yb 18 mol.%.

The obtained dependences reflect the role of cross-relaxation in activator ions. Bands in the regions of 450, 475 and 650 nm are more sensitive to the efficiency of cross-relaxation because they require more photons for excitation than the bands in the regions of 700 and 800 nm.

Appendix

TEM images of the samples.

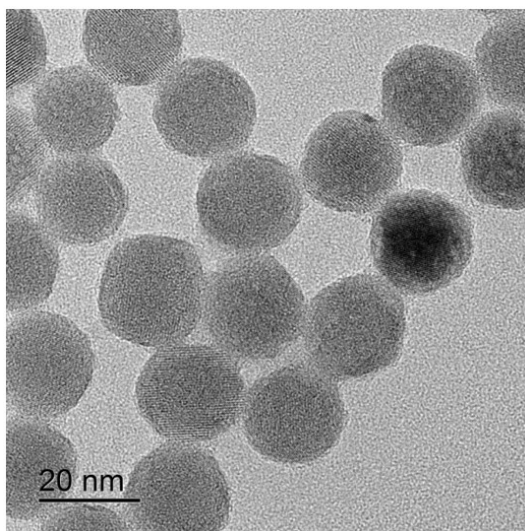


FIG. A1. TEM image of the sample No. 2

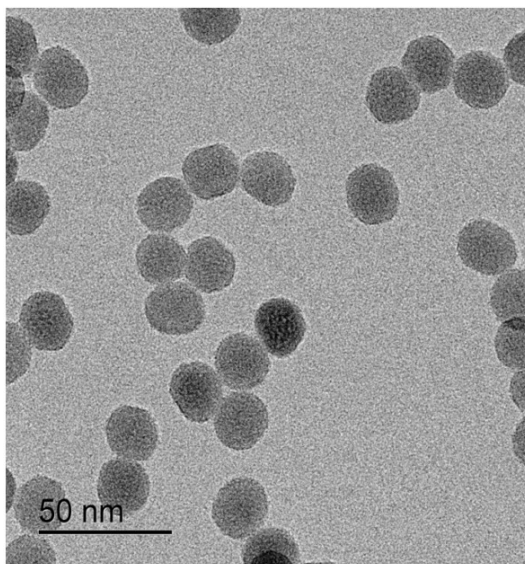


FIG. A2. TEM image of the sample No. 3

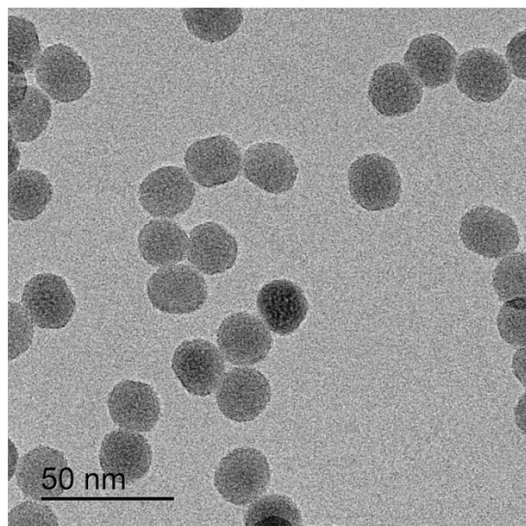


FIG. A3. TEM image of the sample No. 5

Size distribution of nanoluminophores $\beta\text{-NaYF}_4\text{:Yb}^{3+}/\text{Tm}^{3+}$ in DMSO, obtained by DLS method.

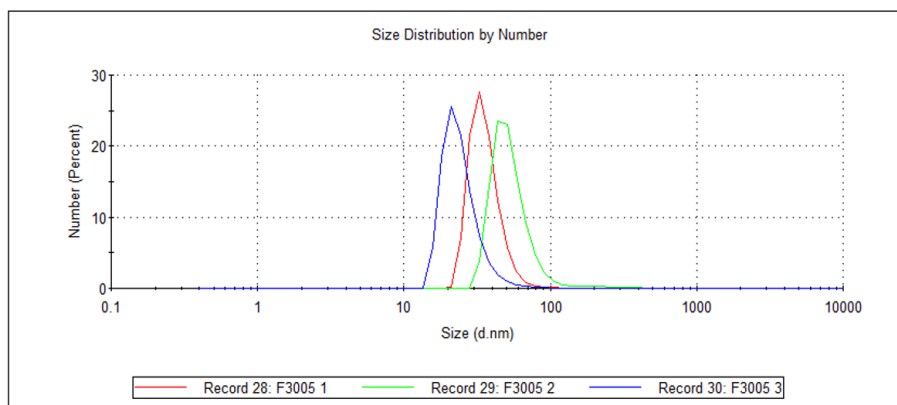


FIG. A4. Size distribution of the sample No. 2

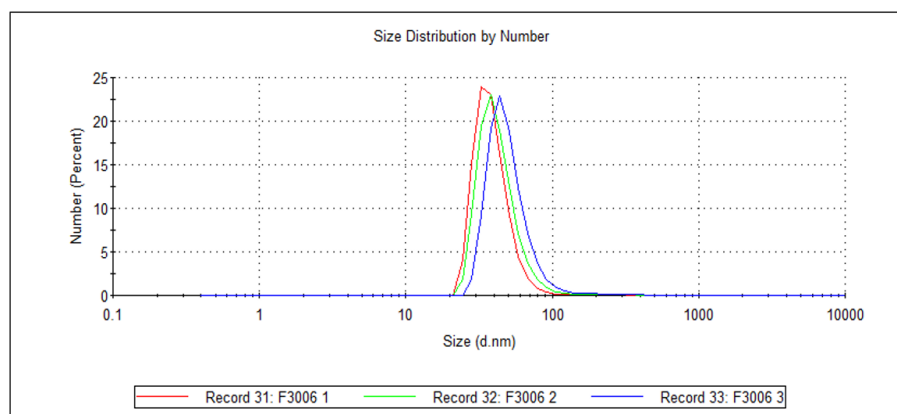


FIG. A5. Size distribution of the sample No. 3

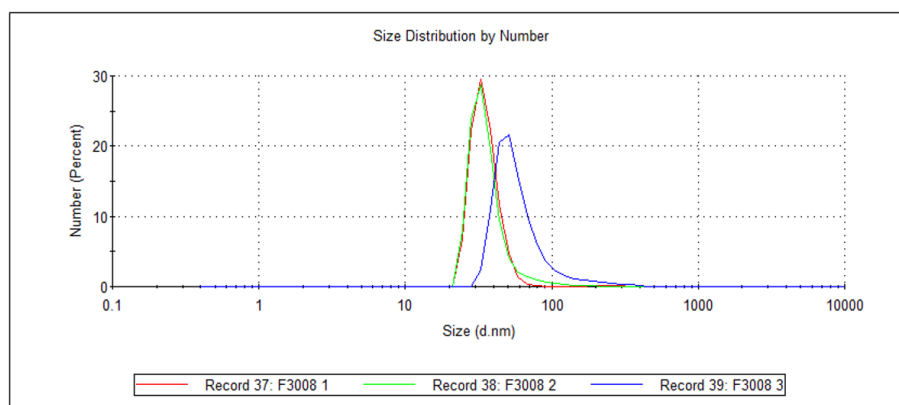


FIG. A6. Size distribution of the sample No. 5

References

- [1] Auzel F. History of upconversion discovery and its evolution. *J. Luminescence*, 2020, **223**, 1169005.
- [2] Bloembergen N. Solid State Infrared Quantum Counters. *Phys. Rev. Lett.*, 1959, **2**, P. 84–85.
- [3] Ovsyankin V.V., Feofilov P.P. Mechanism of Summation of Electronic Excitations in Activated Crystals. *JETP Lett.*, 1966, **3**, P. 322–323.
- [4] Escudero A., Becerro A.I., et al. Rare earth based nanostructured materials: synthesis, functionalization, properties and bioimaging and biosensing applications. *Nanophotonics*, 2017, **6**, P. 881–921.
- [5] Pominova D.V., Proydakova V.Y., et al. Achieving high NIR-to-NIR conversion efficiency by optimization of Tm^{3+} content in $\text{Na}(\text{Gd}, \text{Yb})\text{F}_4$: Tm^{3+} upconversion luminophores. *Laser Physics Letters*, 2020, **17**, 125701.
- [6] Burikov S.A., Kotova O.D., et al. Determining the Photophysical Parameters of NaGdF_4 :Eu Solid Solutions in Suspensions Using the Judd-Ofelt Theory. *JETP Lett.*, 2020, **111**, P. 525–531.
- [7] Liu Q. *Studies of optical properties of lanthanide upconversion nanoparticles for emerging applications*. Stockholm: KTH Royal Institute of Technology, 2020, 73 p.
- [8] Han S., Deng R., Xie X., Liu X. Enhancing luminescence in lanthanide-doped upconversion nanoparticles. *Angew. Chem. Int. Ed.*, 2014, **53**, P. 11702–11715.
- [9] Sarmanova O.E., Burikov S.A., et al. In Vitro Temperature Sensing with Up-Conversion NaYF_4 : Yb^{3+} / Tm^{3+} -Based Nanocomposites: Peculiarities and Pitfalls. *Spectrochim. Acta A*, 2020, **24**, 118627.
- [10] Geitenbeek R.G., Prins P.T., et al. NaYF_4 : Er^{3+} , Yb^{3+} / SiO_2 Core/Shell Upconverting Nanocrystals for Luminescence Thermometry up to 900 K. *J. Phys. Chem. C*, 2017, **121**, P. 3503–3510.
- [11] Jaque D., Vetrone F. Luminescence nanothermometry. *Nanoscale*, 2012, **4**, P. 4301–4326.
- [12] Pominova D., Proydakova V., et al. Temperature sensing in the short-wave infrared spectral region using core-shell NaGdF_4 : Yb^{3+} , Ho^{3+} , Er^{3+} @ NaYF_4 nanothermometers. *Nanomaterials*, 2020, **10** (10), 1992.
- [13] Shalav A., Richards B.S., Green M.A. Luminescent Layers for Enhanced Silicon Solar Cell Performance: Up-Conversion. *Sol. Energy Mater. Sol. Cells*, 2007, **91**, P. 829–842.
- [14] Trupke T., Green M.A., Würfel P. Improving Solar Cell Efficiencies by Up-Conversion of Sub-Band-Gap Light. *J. Appl. Phys.*, 2002, **92**, P. 4117–4122.
- [15] Richards B.S. Enhancing the Performance of Silicon Solar Cells via the Application of Passive Luminescence Conversion Layers. *Sol. Energy Mater. Sol. Cells*, 2006, **90**, P. 2329–2337.
- [16] Hu Y., Sun Y., et al. A facile synthesis of NaYF_4 : Yb^{3+} / Er^{3+} nanoparticles with tunable multicolor upconversion luminescence properties for cell imaging. *RSC Adv.*, 2014, **4**, P. 43653–43660.
- [17] Pilch A., Wawrzyńczyk D., et al. The concentration dependent up-conversion luminescence of Ho^{3+} and Yb^{3+} co-doped β - NaYF_4 . *J. Lumin.*, 2017, **182**, P. 114–122.
- [18] Kormshikov I.D., Voronov V.V., et al. Study of stability of luminescence intensity of β - NaGdF_4 : Yb: Er nanoparticle colloids in water solution. *Nanosystems: Phys. Chem. Math.*, 2021, **12**, P. 218–223.
- [19] Liu H.C., Xu C.T., et al. Balancing power density based quantum yield characterization of upconverting nanoparticles for arbitrary excitation intensities. *Nanoscale*, 2013, **5**, P. 4770–4775.
- [20] Saleta Reig D., Grauel B., et al. Upconversion properties of SrF_2 : Yb^{3+} , Er^{3+} single crystals. *J. Mater. Chem. C*, 2020, **8**, P. 4093–4101.
- [21] Zhao J., Jin D., et al. Single-nanocrystal sensitivity achieved by enhanced upconversion luminescence. *Nature Nanotechnology*, 2013, **8**, P. 729–734.
- [22] Chen G., Ohulchanskyy T.Y., et al. *ACS Nano*, 2010, **4**, P. 3163–3168.
- [23] Ma C.S., Xu X.X., et al. Optimal Sensitizer Concentration in Single Upconversion Nanocrystals. *Nano Lett.*, 2017, **17**, P. 2858–2864.
- [24] Wei W., Zhang Y., et al. Cross relaxation induced pure red upconversion in activator- and sensitizer-rich lanthanide nanoparticles. *Chem. Mater.*, 2014, **26**, P. 5183–5186.
- [25] Pisarenko V.F. Rare-earth scandoborates as new laser materials. *Soros. Obrazovat. Zh.*, 1996, **11**, P. 111–116.
- [26] Li X., Shen D., et al. Successive layer-by-layer strategy for multi-shell epitaxial growth: shell thickness and doping position dependence in upconverting optical properties. *Chem. Mater.*, 2013, **25**, P. 106–112.
- [27] Liu M., GuM., et al. Multifunctional CaSc_2O_4 : Yb^{3+} / Er^{3+} one-dimensional nanofibers: electrospinning synthesis and concentration-modulated upconversion luminescent properties. *J. Mater. Chem. C*, 2017, **5**, P. 4025–4033.
- [28] Bai X., Song H., et al. Size-dependent upconversion luminescence in Er^{3+} / Yb^{3+} -codoped nanocrystalline yttria: saturation and thermal effects. *J. Phys. Chem. C*, 2007, **111**, P. 13611–13617.
- [29] Liu F., Ma E., et al. Tunable red-green upconversion luminescence in novel transparent glass ceramics containing $\text{Er}:\text{NaYF}_4$ nanocrystals. *The Journal of Physical Chemistry B*, 2006, **110**, P. 20843–20846.

- [30] Vetrone F., Boyer J.-C., Capobianco J.A. Significance of Yb³⁺ concentration on the upconversion mechanisms in codoped Y₂O₃:Er³⁺, Yb³⁺ nanocrystals. *J. of Applied Physics*, 2004, **96**, P. 661–667.
- [31] Misiak M., Prorok K., et al. Thulium concentration quenching in the up-converting α -Tm³⁺/Yb³⁺ NaYF₄ colloidal nanocrystals. *Optical Materials*, 2013, **35**, P. 1124–1128.
- [32] Xu D., Liu C., et al. Understanding energy transfer mechanisms for tunable emission of Yb³⁺-Er³⁺ codoped GdF₃ nanoparticles: concentration-dependent luminescence by near-infrared and violet excitation. *J. Phys. Chem. C*, 2015, **119**, P. 6852–6860.
- [33] Tie Cong, Yadan Ding, et al. Solvent-Induced Luminescence Variation of Upconversion Nanoparticles. *Langmuir*, 2016, **32** (49), P. 13200–13206.
- [34] Brites C.D.S., Kuznetsov S.V., et al. Simultaneous measurement of the emission quantum yield and local temperature: The illustrative example of SrF₂:Yb³⁺/Er³⁺ single crystals. *European J. of Inorganic Chemistry*, 2020, **2020** (17), P. 1555–1561.
- [35] Madirov E.I., Konyushkin V.A., et al. Effect of Yb³⁺ and Er³⁺ concentration on upconversion luminescence of co-doped BaF₂ single crystals. *J. Mater. Chem. C*, 2021, **9**, P. 3493–3503.
- [36] Fedorov P.P., Kuznetsov S.V., Osiko V.V. Elaboration of nanofluorides and ceramics for optical and laser applications. In *Photonic & Electronic Properties of Fluoride Materials*, Ed. A. Tressaud, K. Poepelmeier, 2016, P. 7–31.
- [37] Valenta J., Repko A., Greben M., Nižňanský D. Absolute up- and down-conversion luminescence efficiency in hexagonal Na(Lu/Y/Gd)F₄: Yb, Er/Tm/Ho with optimized chemical composition. *AIP Advances*, 2018, **8**, 075226.
- [38] Wang F., Liu X. Upconversion Multicolor Fine-Tuning: Visible to Near-Infrared Emission from Lanthanide-Doped NaYF₄ Nanoparticles. *J. of the American Chemical Society*, 2008, **30**, P. 5642–5643.
- [39] Liu J., Chen G., Hao S., Yang C. Sub-6 nm monodisperse hexagonal core/shell NaGdF₄ nanocrystals with enhanced upconversion photoluminescence. *Nanoscale*, 2017, **9**.
- [40] Clegg R.M. Chapter 1 Förster resonance energy transfer – FRET what is it, why do it, and how it's done. *Laboratory Techniques in Biochemistry and Molecular Biology*, 2009, **33**, P. 1–57.
- [41] Dexter D.L. A Theory of Sensitized Luminescence in Solids. *J. Chem. Phys.*, 1953, **21**, P. 836–850.
- [42] Bergstrand J., Liu Q.Y., et al. On the decay time of upconversion luminescence. *Nanoscale*, 2019, **11**, P. 4959–4969.
- [43] Wen S., Zhou J., et al. Advances in highly doped upconversion nanoparticles. *Nat. Commun.*, 2018, **9**, 2415.

Submitted 5 May 2022; accepted 14 June 2022

Information about the authors:

Sergey V. Kuznetsov – Prokhorov General Physics Institute of the Russian Academy of Sciences, Moscow, 119991, Russia; ORCID 0000-0002-7669-1106; kouznetzovsv@gmail.com

Sergey A. Burikov – Department of Physics, Lomonosov Moscow State University, Moscow, 119991, Russia; ORCID 0000-0003-2271-8980; sergey.burikov@gmail.com

Anna A. Fedyanina – Department of Physics, Lomonosov Moscow State University, Moscow, 119991, Russia; ORCID 0000-0001-6659-5674; fedyanechka@mail.ru

Ekaterina A. Filippova – Department of Physics, Lomonosov Moscow State University, Moscow, 119991, Russia; filippova.ea17@physics.msu.ru

Vera Yu. Proydakova – Prokhorov General Physics Institute of the Russian Academy of Sciences, Moscow, 119991, Russia; ORCID 0000-0001-8017-9175; vera.proydakova@gmail.com

Valerii V. Voronov – Prokhorov General Physics Institute of the Russian Academy of Sciences, Moscow, 119991, Russia; ORCID 0000-0001-5029-8560; voronov@lst.gpi.ru

Nataliya Yu. Tabachkova – Prokhorov General Physics Institute of the Russian Academy of Sciences, Moscow, 119991, Russia; ORCID 0000-0002-0169-5014; ntabachkova@gmail.com

Pavel P. Fedorov – Prokhorov General Physics Institute of the Russian Academy of Sciences, Moscow, 119991, Russia; ORCID 0000-0002-2918-3926; ppfedorov@yandex.ru

Tatiana A. Dolenko – Department of Physics, Lomonosov Moscow State University, Moscow, 119991, Russia; ORCID 0000-0003-2884-8241; tdolenko@mail.ru

Conflict of interest: the authors declare that they have no known competing financial interests or personal relationships that could have appeared to influence the work reported in this paper.